

Accepted Manuscript

Characterisation of Screen-Printed Gold and Gold Nanoparticle-Modified Carbon Sensors by Electrochemical Impedance Spectroscopy

Elena Bernalte, Carmen Marín-Sánchez, Eduardo Pinilla-Gil, Christopher M.A Brett

PII: S1572-6657(13)00414-1

DOI: <http://dx.doi.org/10.1016/j.jelechem.2013.09.007>

Reference: JEAC 1401

To appear in: *Journal of Electroanalytical Chemistry*

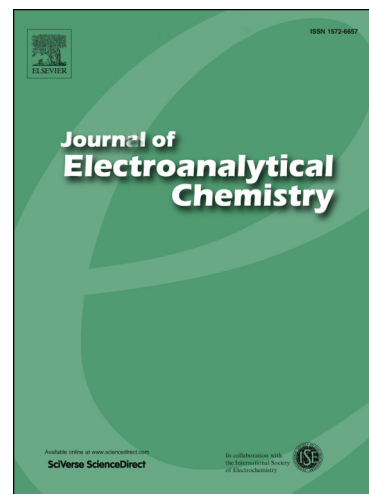
Received Date: 11 June 2013

Revised Date: 13 September 2013

Accepted Date: 14 September 2013

Please cite this article as: E. Bernalte, C. Marín-Sánchez, E. Pinilla-Gil, C.M. Brett, Characterisation of Screen-Printed Gold and Gold Nanoparticle-Modified Carbon Sensors by Electrochemical Impedance Spectroscopy, *Journal of Electroanalytical Chemistry* (2013), doi: <http://dx.doi.org/10.1016/j.jelechem.2013.09.007>

This is a PDF file of an unedited manuscript that has been accepted for publication. As a service to our customers we are providing this early version of the manuscript. The manuscript will undergo copyediting, typesetting, and review of the resulting proof before it is published in its final form. Please note that during the production process errors may be discovered which could affect the content, and all legal disclaimers that apply to the journal pertain.



1 **CHARACTERISATION OF SCREEN-PRINTED GOLD AND GOLD NANOPARTICLE-MODIFIED**
2 **CARBON SENSORS BY ELECTROCHEMICAL IMPEDANCE SPECTROSCOPY**

3 **Elena Bernalte^{1,*}, Carmen Marín-Sánchez¹, Eduardo Pinilla-Gil¹, Christopher M.A Brett²**

4 ¹*Departamento de Química Analítica, Universidad de Extremadura, Avda. de Elvas, s/n, E-*
5 *06006 Badajoz, Spain*

6 ²*Departamento de Química, Faculdade de Ciências e Tecnologia, Universidade de Coimbra,*
7 *3004-535 Coimbra, Portugal*

8 *ebernalte@unex.es*

9 *Phone: +34-924-289392*

10 *Fax: +34-924-274244*

11 **Abstract**

12 Gold-based screen-printed electrodes have been characterised by electrochemical impedance
13 spectroscopy (EIS) to better understand their behaviour in electroanalytical applications,
14 particularly in the anodic stripping voltammetry of Hg(II). After a first exploration by cyclic
15 voltammetry, impedance spectra of gold-based screen-printed sensors were recorded in 0.1 M
16 HCl electrolyte solution, in the presence of dissolved oxygen and with no electrochemical pre-
17 treatment of the surface. The spectra demonstrated the differences in the interfacial
18 characteristics of each kind of sensor. Structural changes in the surface of SPGEs caused by
19 amalgam formation in the presence of Hg(II) were investigated by EIS. The results obtained
20 were used to elucidate the implications for using the sensor in the stripping voltammetric
21 determination of Hg(II) in environmental samples.

22 **Keywords:** Gold-based screen-printed electrodes; EIS; Hg

23 **1. Introduction**

24 The increasing availability of low-price homemade and commercial screen-printed
25 electrochemical platforms has opened up new and exciting opportunities to apply
26 electrochemical techniques outside a centralised laboratory [1-3], reinforcing one of the most
27 important trends in analytical chemistry, and especially environmental monitoring, towards
28 miniaturized, portable devices for on-site or even *in situ* application [4]. In this context, the
29 great utility and versatility presented by screen-printed electrodes (SPEs) lies in the wide range
30 of ways in which the disposable strips may be employed, as reviewed by Domínguez-Renedo et
31 al. [5].

32 Despite the wide practical application of SPEs, little is known about the nature of electrode
33 reactions at their complex surface [6]. Differences in the composition of commercial printing
34 inks, diverse pre-treatment procedures and variable temperature conditions during the curing
35 of the printing layer can affect their electrochemical behaviour; several studies have been
36 performed with the aim of their characterisation [4, 6-8]. In these papers, cyclic voltammetry
37 (CV), pulse techniques such as square wave voltammetry (SWV) and scanning electron
38 microscopy (SEM) were used for this purpose. Changes in the sensing interfacial region of the
39 electrodes may not be observed by CV or SWV. However, they are observable by
40 electrochemical impedance spectroscopy (EIS), owing to the wide range of timescales that this

41 technique probes [9]. EIS has been demonstrated as a powerful tool for electrochemical
42 characterization [10-14].

43 In previous work, we have successfully demonstrated the applicability of screen printed gold
44 electrodes (SPGE) and gold nanoparticle modified screen-printed carbon electrodes (GNP) for
45 Hg(II) monitoring in different environmental samples [2, 15-17]. As widely described, gold is
46 the best electrode material for the electroanalytical determination of mercury, but it presents
47 an important drawback that is the well-known phenomenon of structural changes of the
48 surface, caused by amalgam formation with mercury [15].

49 Therefore, the aim of the present work was to characterise, by cyclic voltammetry and
50 electrochemical impedance spectroscopy, three types of commercial screen-printed
51 electrodes: high and low temperature cured screen-printed gold electrodes (SPGE-AT, SPGE-
52 BT) and gold nanoparticles-modified screen-printed carbon electrodes (GNP). Also, the surface
53 of SPGE-AT were also characterised by EIS in presence of Hg(II) to evaluate the influence of
54 amalgam formation. Finally, the observation and characterisation of the gold working
55 electrodes surfaces were also carried out by scanning electron microscopy (SEM) and X-ray
56 photoelectron spectroscopy (XPS).

57 2. Experimental

58 2.1. Reagents and solutions

59 All stock and standard solutions were made from analytical grade reagents. A 10 mg/L stock
60 solution of Hg(II) was supplied by PerkinElmer (Spain) and working solutions were prepared
61 before measurements by dilution with ultrapure water (resistivity > 18.2 M Ω ·cm at 25 °C)
62 obtained from an Ultramatic system (Wasserlab, Spain). The supporting electrolyte was 0.1 M
63 HCl (Panreac, Spain) that was demonstrated to be suitable for ASV measurements of mercury
64 [2, 15-17]. The glassware and electrochemical cell were thoroughly conditioned by cleaning
65 with hot nitric acid (10 %), rinsing with ultrapure water, drying, and keeping in hermetic plastic
66 bags before use.

67 Experiments were conducted at room temperature (25 \pm 1 °C) without deoxygenation.

68 2.2. Electrodes and electrochemical cell

69 Screen-printed electrodes (models 220AT, 220BT, and 110GNP) were purchased from
70 DropSens (Oviedo, Spain). They were designed in a three electrode configuration constructed
71 on the same ceramic platform. Working electrodes ($A_{\text{geom}} = 0.126 \text{ cm}^2$) were composed of
72 carbon, high and low temperature curing gold inks, and gold nanoparticles-on-carbon,
73 respectively. Ink formulation and production characteristics of commercial SPEs are regarded
74 by the manufacturers as proprietary information. In all of them counter and pseudo-reference
75 printed electrodes were made of carbon (in GNP) or gold (in SPGE 220AT and 220BT), and
76 silver, respectively. An insulating layer served to delimit the working area and silver electrical
77 contacts of the electrode strips, connected by a special electrical connector to the
78 potentiostat. A methacrylate voltammetric cell (DropSens, Spain) was used to perform
79 voltammetric and EIS measurements. It is especially suitable for SPEs and designed to perform
80 batch analysis with volumes of solution between 5 and 10 mL, with optional stirring by means

81 of a magnetic stirrer. The screen-printed strips were immersed in the solution through a slit in
82 the top lid leaving the electrical connections outside.

83 2.3. Instrumentation and methods

84 Voltammetric experiments were performed on a computerized hand-held, battery-powered
85 PalmSens potentiostat/galvanostat (Palm Instruments BV, The Netherlands) interfaced with a
86 laptop and controlled by the PalmSens PC software (PS Trace 2.5.2.0). For square-wave anodic
87 stripping voltammetry (SWASV) the conditioning potential was +0.70 V for 15 s, deposition
88 potential +0.20 V for 60 s, amplitude 40 mV, step potential 6 mV, frequency 20 Hz,
89 equilibration time 10 s, and stirring rate 600 rpm [15].

90 Electrochemical impedance spectra were recorded using a CH Instruments 660D equipment
91 controlled by the software provided by the supplier (CH Instruments, Inc., USA) or a Solartron
92 1250 Frequency Response Analyser coupled to a Solartron 1286 Electrochemical Interface
93 (Solartron Analytical, UK), controlled by ZPlot software. The frequency range from 65 kHz to
94 0.1 Hz was scanned logarithmically with an applied sinusoidal perturbation of 10 mV rms
95 amplitude in 12 steps per frequency decade, superimposed on the chosen applied potential.
96 Data fitting to equivalent circuits was performed with CHI analyzer program and ZView
97 software, respectively. Four replicates were done at each value of applied potential to verify
98 reproducibility of the responses.

99 SEM images of the working electrode surfaces were obtained by using a Hitachi FE-SEM S-
100 4800II field emission scanning electron microscope (Tokyo, Japan). A K-Alpha X-ray
101 photoelectron spectrometer (XPS) system (Thermo Scientific, USA) was used for X ray surface
102 analysis of the SPEs.

103 3. Results and discussion

104 The electrochemical characterisation of the high and low temperature cured screen-printed
105 gold electrodes (SPGE-AT, SPGE-BT) and gold nanoparticle-modified screen-printed carbon
106 electrodes (GNP) were done by cyclic voltammetry and electrochemical impedance
107 spectroscopy. Observation and characterisation of the working electrode surfaces were carried
108 out by SEM and XPS, which provided morphological and microstructural information. The
109 principal results will be discussed below.

110 3.1. Electrochemical characterisation of the SPEs

111 3.1.1. Cyclic voltammetry

112 The behaviour of bare screen-printed electrodes was first investigated by cyclic voltammetry
113 (CV) in order to examine their potential window and the magnitude of the background
114 currents. The information obtained was also used to establish the applied potentials to be
115 used in the subsequent impedance experiments.

116 Cyclic voltammograms were recorded in 0.1 M HCl solution without pre-treatment of the
117 working electrode surface. As expected, differences in the potential windows between
118 different types of SPEs were significant (Figure 1). The width of the potential windows

119 decreased in the following order: GNP (1.9 V)>SPGE-BT (1.4 V)>SPGE-AT (1.2 V). In all SPEs, the
120 positive potential limit remains stable around +0.8 V but the negative potential limit shifts to
121 more positive values as the proportion of exposed gold increases. Additionally, the background
122 current was significantly higher for SPGE-AT. The percentage of carbon present in the
123 composition of the surface of working electrodes, as revealed by XPS: (GNP (69.9 %C)>SPGE-BT
124 (68.0 %C)>SPGE-AT (27.5 %C), shows that the changes in the negative potential limit can be
125 attributed to the amount of gold and carbon exposed as well as the dispersion over the
126 electrode surface.

127 Cyclic voltammograms of GNP (Figure 1C) present the typical behaviour of carbon electrodes.
128 However, cyclic voltammograms of SPGE-BT (Figure 1B) and SPGE-AT (Figure 1A) show an
129 unusual peak in the positive sweep around 0.0 V, probably due to an interferent species that
130 could be part of the gold ink formulation. Thus, square wave anodic stripping voltammograms
131 of 0.1 M HCl solutions were recorded and the results are also shown in Figure 1. As can be
132 observed, the same peak at 0.1 V appeared for the three types of SPE. On the other hand,
133 another peak appeared at 0.0 V in the stripping voltammogram of GNP, and also of SPGE-BT
134 but with lower intensity, probably due to an oxidative process of the carbon-based film.
135 However, the highest signal measured was observed at -0.1 V in the stripping voltammograms
136 of SPGE-AT, that could probably be attributed to the presence of an unknown substance
137 involved in the manufacturing of SPGE. This is in agreement with an observation reported
138 previously [15] in which it was demonstrated that SPGE-AT could only be used at positive
139 potentials, because irreversible changes occurred on the surface of the working electrode at
140 negative potentials.

141 Based on these considerations and taking into account that the application of the SPEs is
142 focused on Hg(II) determination by SWASV, the potentials selected for recording impedance
143 spectra were 0.0 V (initial potential without interference signals), 0.2 V (potential for
144 deposition of Hg in SWASV) [2], 0.4 (stripping peak potential of Hg by SWASV) [2, 15-17] and
145 0.7 V (final potential).

146 3.1.2. Electrochemical impedance spectroscopy

147 Experimental complex plane impedance spectra for the bare SPGE-AT, SPGE-BT, and GNP are
148 shown in Figure 2 together with fitting to equivalent circuits. As seen in Figure 2, the shape of
149 the impedance spectra depends on the applied potential. The almost linear and close-to-
150 vertical spectra at 0.2 V and 0.4 V indicate a purely capacitive response (with effects of surface
151 non-uniformity) in contrast to the semicircular complex plane plots obtained at 0.0 V and 0.7
152 V, where both resistive and capacitive elements are important. The differences between the
153 types of SPE are more clearly observed in the complex plane plots obtained at 0.0 V and 0.7 V.

154 Fitting of spectra was done using one of the three equivalent electrical circuits shown in Figure
155 3, the first two of these being simplifications of the third circuit. R_{Ω} represents the cell
156 resistance, R_1 and R_2 are resistances, and CPE_1 and CPE_2 are constant phase elements
157 modelling non-ideal capacitors of capacity C_1 or C_2 . The CPE exponent α represents the
158 roughness and non-uniformity of the electrode surface, an α value of 1 corresponding to a
159 perfectly smooth surface and of 0.5 to a porous electrode [11]. The CPEs were necessary due
160 to the depressed semi-circle character of the responses. The results obtained are shown in

161 Table 1. Good fits were obtained and low relative errors were found for all parameters, always
162 less than 5 %. Placing the two RCPE in parallel did not give good fitting to the experimental
163 data. Thus, this circuit model can be attributed to the ink used – see further below. In general
164 terms, the couple R_1CPE_1 would represent the surface layers of the film, and R_2CPE_2 charge
165 transfer processes and double layer at the electrode-solution interface. Thus, at intermediate
166 potentials where there are no charge transfer processes, the circuits in Fig.3a or 3b can be
167 employed, whereas at 0.7 V where surface oxidation can occur, it is necessary to employ the
168 full circuit of Fig.3c, and at 0.0 V (reduction process) for SPGE-AT.

169 Similar values of the cell resistance, R_Ω , of around $3 \Omega \text{ cm}^2$ were observed for SPGE-AT and
170 SPGE-BT at all applied potentials tested, in contrast to the higher values of nearly $60 \Omega \text{ cm}^2$
171 obtained for GNP, that must be mainly due to the resistance of the carbon ink (SPCE gives 30Ω
172 cm^2) and areas of the electrode surface which become less conducting after gold nanoparticle
173 deposition. As seen in Table 1, immobilisation of gold nanoparticles on the surface of screen-
174 printed carbon electrodes, gives a value of R_1 higher by a factor of a hundred, and a lower
175 capacitance (CPE_1). The increase in R_1 can indicate a partially blocked surface with adsorbed
176 gold nanoparticles.

177 A priori, the necessity of fitting using the full circuit of Fig.3c is unexpected for SPGE-AT solid
178 gold screen-printed electrodes for which high temperature curing of the ink is used (it is not
179 needed for SPGE-BT, which has low-temperature curing). In agreement with the results
180 obtained from cyclic voltammetry and anodic stripping voltammetry, this behaviour of SPGE-
181 AT could be due to the presence of some interference involved in the printing ink
182 manufacturing process (proprietary information).

183 The values of α for SPGE-AT, SPGE-BT and GNP were all around 0.9, suggesting a low degree of
184 non-uniformity. The tendency for slightly lower values of α (~ 0.87) for SPGE-BT may be due to
185 the influence of the low temperature gold curing process on the structural characteristics of
186 the electrode. Figure 4 presents SEM images obtained for SPGE-AT and SPGE-BT, to illustrate
187 the differences in the surface morphology and structure of the gold working electrodes after
188 the ink curing process. The microscopic images of SPGE-BT show a significantly greater
189 roughness that can explain the different values of the α exponent.

190 3.2. Impedance in the presence of Hg(II)

191 As widely described in the literature, the principal drawback of the electrochemical
192 determination of Hg(II) using solid gold electrodes is the well-known structural change of the
193 surface due to amalgam formation with mercury. Consequently, after the stripping
194 voltammetric determination, the memory effect caused by amalgamation demands extensive
195 electrochemical cleaning to recover low background currents in subsequent measurements.
196 Therefore, electrochemical impedance spectroscopy was used to examine the reversible
197 and/or irreversible alterations in SPGE-AT behaviour after performing SWASV in the presence
198 of Hg(II).

199 The experiments were performed as follows: 10 repeated SWASV measurements, without any
200 cleaning step between measurements, in the presence of 10, 20, or 50 ng/mL of Hg(II) were

201 carried out successively. After that, impedance spectra (4 replicates) were recorded at 0.0 V,
202 0.2 V, 0.4 V, and 0.7 V, in 0.1 M HCl.

203 After SWASV experiments with mercury, there are changes to the surface as can be inferred,
204 not only from visual examination of the complex plane spectra but also from the change in the
205 equivalent circuit needed for fitting and the values of the parameters obtained. Spectra
206 obtained for SPGE-AT are shown in Figure 5 and the analysis of the results is given in Table 2,
207 fitting done with an equivalent circuit consisting of a cell resistance in series with only one
208 parallel RCPE rather than two (0.0 and 0.7 V) or CPE (0.2 and 0.4 V), Fig.3a and 3b. No
209 significant overall changes in the magnitude of the impedances were observed after SWASV of
210 Hg(II) (compare data in Tables 1 and 2), and therefore that the amalgamation of Hg with the
211 gold working electrode does not cause any big structural changes in the surface layers of SPGE.
212 However, some alterations must occur in the presence of metal ion, since the best equivalent
213 circuit for modelling has just one RCPE, in contrast to the 2 RCPEs needed without mercury at
214 0.0 and 0.7 V. It is also seen that an increase of charge transfer resistance and a decrease of
215 CPE occur after analysing 50 ng/mL of Hg(II), whereas lower concentrations of Hg(II) did not
216 affect these parameters. Despite the fact that no irreversible changes take place at the surface
217 of SPGE in the presence of low concentrations of Hg, it is seen that a relatively high
218 concentration of the analyte (50 ng/mL) can modify the surface of the electrode, since access
219 to the electrode is partially blocked by the amalgamation of Hg with gold, as shown in Table 2.
220 These observations also suggest that excessive metal deposition may lead to removal of the
221 gold surface layers and thence loss of accuracy and reproducibility of the responses.

222 4. Conclusions

223 Screen-printed electrodes based on gold cured at high (SPGE-AT) and low (SPGE-BT)
224 temperature and carbon-modified with gold nanoparticles (GNP), were characterised by EIS.
225 Cyclic voltammetry was used to establish the optimal potential values for performing EIS
226 experiments.

227 EIS data show evidence of the differences in the behaviour of the screen-printed sensors at the
228 different potentials monitored. GNP shows an increase in the magnitude of the charge transfer
229 resistance and a decrease of capacitance indicating a partially blocked surface with gold
230 nanoparticles which hinder the electron transfer. In agreement with the observations from CV,
231 EIS results obtained for SPGE-AT can be related to the printing ink manufacturing process.

232 No significant changes to the surface of SPGE-AT caused by Hg(II) deposition by SWASV were
233 demonstrated by EIS. However, the disorder caused in the surface of the electrode by
234 deposition of a relatively high concentration of Hg(II) is manifested in the impedance spectra.

235 This approach based on the application of impedance spectroscopy is very useful for studying
236 the behaviour and the properties of the gold-based screen-printed electrodes employed for *in*
237 *situ* monitoring of mercury in the environment.

238 Acknowledgements

239 This work is supported by the Spanish Ministry of Science and Innovation (project CTQ2011-
240 25388). The authors thank the technical and human support provided by Facility of Analysis

241 and Characterization of Solids and Surfaces of SAIUEx (financed by UEx, Gobierno de
242 Extremadura, MICINN, FEDER and FSE) for their assistance with SEM and XPS. E. Bernalte
243 acknowledges a grant from Gobierno de Extremadura, Spain (PRE09107). Financial support
244 from Fundação para a Ciência e Tecnologia (FCT), Portugal, project PTDC/QUI-
245 QUI/116091/2009, and PEst-C/EME/UI0285/2013, POPH (co-financed by the European
246 Community Funds FSE and FEDER/COMPETE–Programa Operacional Factores de
247 Competitividade), is gratefully acknowledged.

248 *References*

249 [1] J. P. Metters, R. O. Kadara, C. E. Banks. New directions in screen printed electroanalytical
250 sensors: an overview of recent developments. *Analyst* 136 (2011) 1067.

251 [2] E. Bernalte, C. Marín Sánchez, E. Pinilla Gil. Gold nanoparticles-modified screen-printed
252 carbon electrodes for anodic stripping voltammetric determination of mercury in ambient
253 water samples. *Sensor. Actuat. B-Chem* 161 (2012) 669.

254 [3] M. Li, Y-T. Li, D-W. Li, Y-T. Long. Recent developments and applications of screen-printed
255 electrodes in environmental assays-A review. *Anal. Chim. Acta* 734 (2012) 31.

256 [4] R. García-González, M. T. Fernández-Abedul, A. Pernía, A. Costa-García. Electrochemical
257 characterization of different screen-printed gold electrodes. *Electrochim. Acta* 53 (2008) 3242.

258 [5] O. Domínguez-Renedo, M. A. Alonso-Lomillo, M.J. Arcos-Martínez. Recent developments in
259 the Field of screen-printed electrodes and their related applications. *Talanta* 73 (2007) 202.

260 [6] P. Fanjul-Bolado, D. Hernández-Santos, P. J. Lamas-Ardisana, A. Martín-Pernía, A. Costa-
261 García. Electrochemical characterization of screen-printed and conventional carbon paste
262 electrodes. *Electrochim. Acta* 53 (2008) 3635.

263 [7] R. O. Kadara, N. Jenkinson, C. E. Banks. Characterisation of commercially available
264 electrochemical sensing platforms. *Sensor. Actuat. B-Chem.* 138 (2009) 556.

265 [8] R. O. Kadara, N. Jenkinson, C. E. Banks. Characterization and fabrication of disposable
266 screen printed microelectrodes. *Electrochem. Commun.* 11 (2009) 1377.

267 [9] C. M. A. Brett. Electrochemical impedance spectroscopy for characterization of
268 electrochemical sensors and biosensors. *ECS Transactions*, **13**(13) (2008) 67.

269 [10] C. Gouveia-Caridade, C. M. A. Brett. Electrochemical impedance characterization of
270 nafion-coated carbon film resistor electrodes for electroanalysis. *Electroanalysis* 17 (2005) 549.

271 [11] C. Gouveia-Caridade, C. M. A. Brett. The influence of Triton-X-100 surfactant on the
272 electroanalysis of lead and cadmium at carbon film electrodes-An electrochemical impedance
273 study. *J Electroanal. Chem.* 592 (2006) 113.

274 [12] A. P. P. Ferreira, C. S. Fugivara, S. Barrozo, P. H. Suegama, H. Yamanaka, A. V. Benedetti.
275 Electrochemical and spectroscopic characterization of screen-printed gold-based electrodes
276 modified with self-assembled monolayers and Tc85 protein. *J Electroanal. Chem.* 634 (2009)
277 111.

- 278 [13] A. Bonanni, M. Pumera, Y. Miyahara. Influence of gold nanoparticles size (2-50 nm) upon
279 its electrochemical behavior: an electrochemical impedance spectroscopic and voltammetric
280 study. *Phys. Chem. Chem. Phys.* 13 (2011) 4980.
- 281 [14] A. Mandil, R. Pauliukaite, A. Amine, C. M. A. Brett. Electrochemical characterization of and
282 stripping voltammetry at screen-printed electrodes modified with different brands of multiwall
283 carbon nanotubes and bismuth films. *Anal. Lett.* 45 (2012) 395.
- 284 [15] E. Bernalte, C. Marín Sánchez, E. Pinilla Gil. Determination of mercury in ambient water
285 samples by anodic stripping voltammetry on screen-printed gold electrodes. *Anal. Chim. Acta*
286 689 (2011) 60.
- 287 [16] E. Bernalte, C. Marín Sánchez, E. Pinilla Gil. Determination of mercury in indoor dust
288 samples by ultrasonic probe microextraction and stripping voltammetry on gold nanoparticles-
289 modified screen-printed electrodes. *Talanta* 97 (2012) 187.
- 290 [17] E. Bernalte, C. Marín Sánchez, E. Pinilla Gil. High-throughput mercury monitoring in indoor
291 dust microsamples by bath ultrasonic extraction and anodic stripping voltammetry on gold
292 nanoparticles-modified screen-printed electrodes. *Electroanalysis* 25 (2013) 289.

293 *Figure captions*

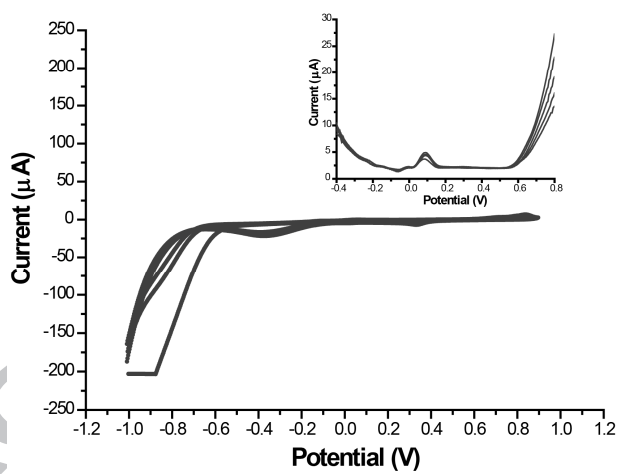
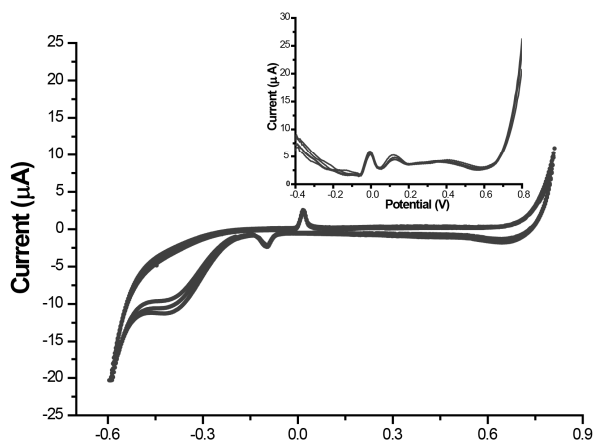
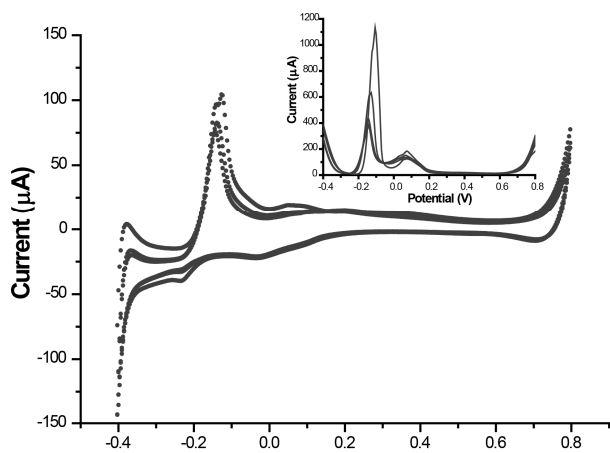
294 Figure 1. Cyclic voltammograms in 0.1 M HCl at A) SPGE-AT, B) SPGE-BT, and C) GNP. Scan rate
295 100 mVs^{-1} . Inset: square-wave anodic stripping voltammograms of 0.1 M HCl solutions. SWASV
296 conditions: frequency 20 Hz, step potential 6 mV, amplitude 40 mV, and deposition time 60 s.
297 Initial and final potentials were -0.4V and 0.7V, respectively.

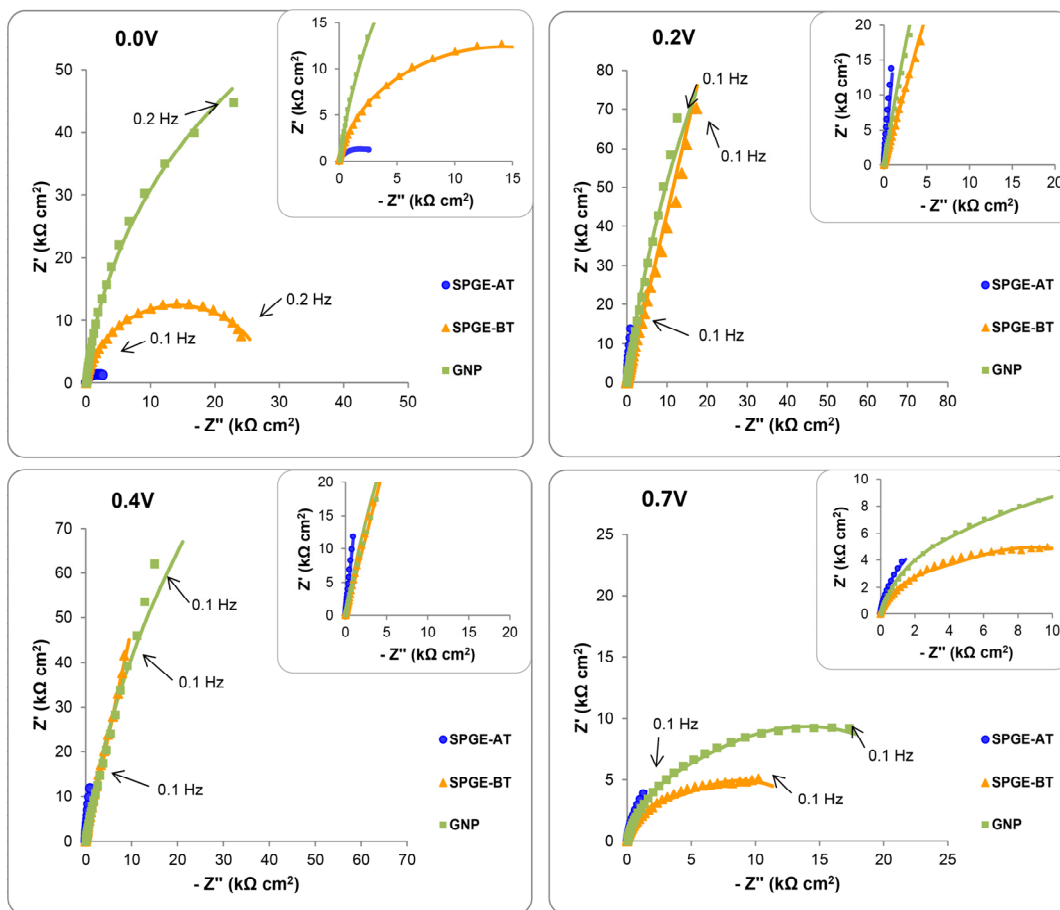
298 Figure 2. Complex plane impedance spectra at 0.0, 0.2, 0.4, and 0.7 V (vs. pseudo Ag/AgCl) for
299 SPGE-AT, SPGE-BT, and GNP in 0.1 M HCl. Inset plots: magnification of “high” frequency part of
300 complex plane plots. Lines represent fitting to the equivalent circuits described in Fig.3 and
301 Tables 1 and 2.

302 Figure 3. Equivalent circuits for fitting impedance spectra at different applied potentials

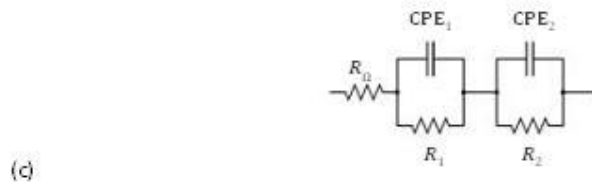
303 Figure 4. SEM images obtained for (A) SPGE-AT and (B) SPGE-BT.

304 Figure 5. Complex plane impedance plots at 0.0, 0.2, 0.4, and 0.7 V (vs. pseudo Ag/AgCl) for
305 SPGE-AT in 0.1 M HCl after SW measurements in the presence of 10, 20, and 50 ng/mL Hg(II)





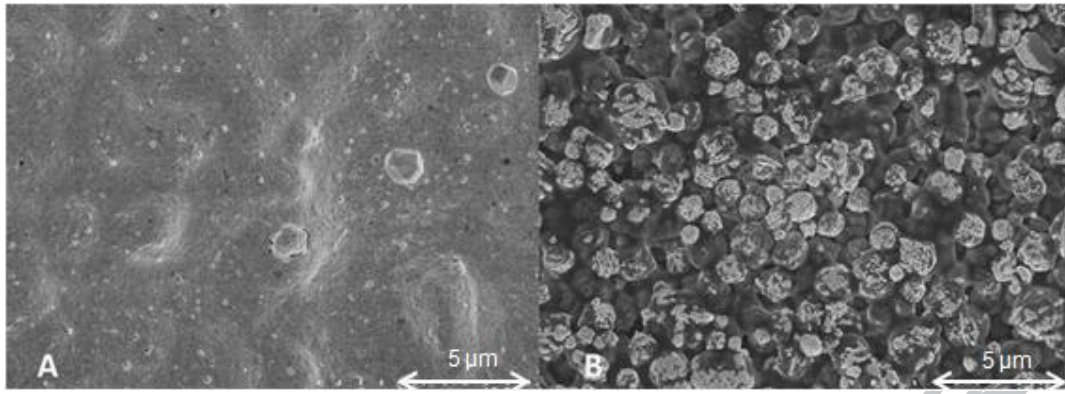
307

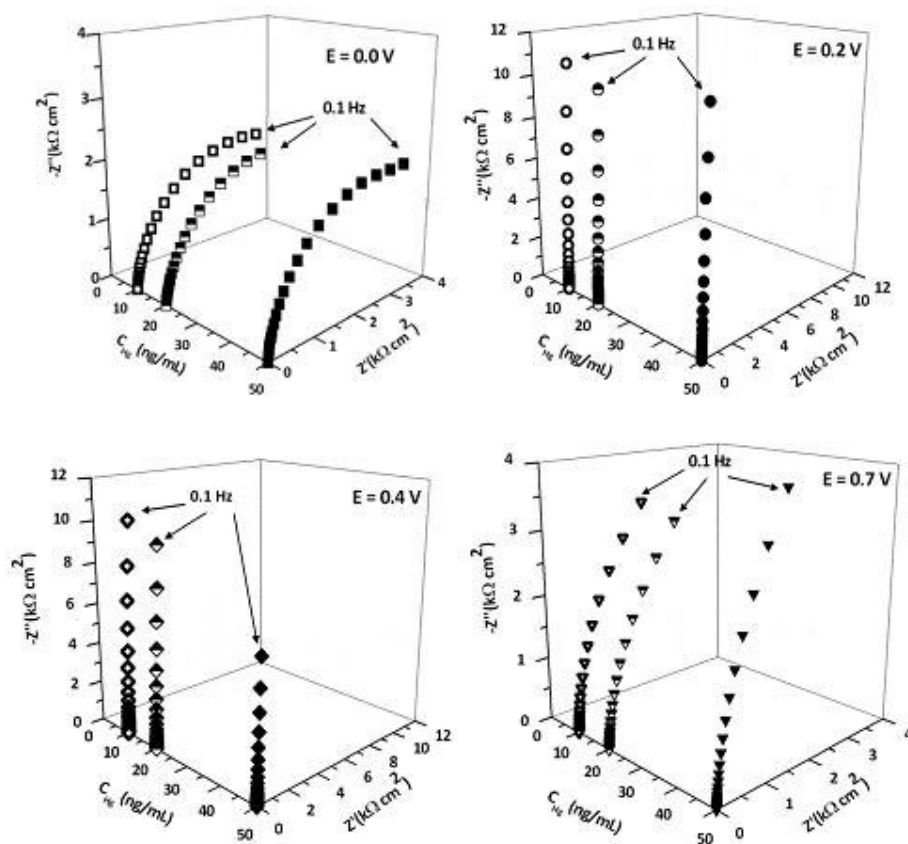


308

ACCEPTED MANUSCRIPT

309





310

311 Table 1. Data obtained from analysis of the impedance spectra for SPGE-AT, SPGE-BT, and GNP
 312 in 0.1 M HCl and in the absence of oxygen

Electrode	E (V) (vs. Pseudo Ag/AgCl)	R_{Ω} (Ω cm^2)	CPE_1 ($\mu\text{S cm}^{-2} \text{s}^{\alpha}$)	α_1	R_1 ($\text{k}\Omega$ cm^2)	CPE_2 ($\mu\text{S cm}^{-2} \text{s}^{\alpha}$)	α_2	R_2 ($\text{k}\Omega \text{cm}^2$)	Error (%)
SPGE-AT	0.0	2.8	1033	0.84	4.1	211	0.89	1.93	2.1
	0.2	2.9	118	0.95					5.1
	0.4	2.9	136	0.95					5.5
	0.7	2.7	343	0.96	16.4	4133	0.71	0.002	1.4
SPGE-BT	0.0	3.0	12.6	0.91	22.3				2.1
	0.2	2.9	18.4	0.86					3.1
	0.4	3.3	32.9	0.87					5.8
	0.7	3.0	30.3	0.87	4.0	91.0	0.87	10.73	3.6
GNP	0.0	56	23.7	0.90	140				2.9
	0.2	57	19.8	0.93	678				3.9
	0.4	57	19.6	0.92	440				4.3
	0.7	56	43.5	0.92	26.4	34.8	0.95	5.44	2.6

313

314

315 Table 2. Data obtained from analysis of the impedance spectra for SPGE-AT in 0.1 M HCl after
 316 SWASV measurements in the presence of 10, 20, and 50 ng/mL of Hg(II)

[Hg(II)] (ng/mL)	E (V) (vs. pseudoAg/AgCl)	R_{Ω} ($\Omega \text{ cm}^2$)	CPE_1 ($\mu\text{S cm}^{-2} \text{ s}^{\alpha}$)	α_1	R_1 ($\text{k}\Omega \text{ cm}^2$)	Error (%)
10	0.0	2.6	168	0.93	4.4	4-8
	0.2	2.6	145	0.98		
	0.4	2.6	152	0.98		
	0.7	2.5	370	0.97	10.6	
20	0.0	2.5	233	0.92	4.3	4-8
	0.2	2.5	157	0.98		
	0.4	2.5	164	0.98		
	0.7	2.5	385	0.97	9.1	
50	0.0	2.6	170	0.94	4.4	4-8
	0.2	2.6	148	0.98		
	0.4	2.6	156	0.98		
	0.7	2.6	337	0.97	13.8	

317

318

319 Highlights

320 - We report the first characterisation of screen-printed gold-based electrodes.

321 - We monitor the influence of amalgam formation after SW determination of Hg.

322 - Structural changes of the surface of the SPEs are studied by EIS.

323

ACCEPTED MANUSCRIPT